Hemodynamic Environments from Opposing Sides of Human Aortic Valve Leaflets Evoke Distinct Endothelial Phenotypes In Vitro

Cardiovasc Eng (2010) 10:5–11
DOI 10.1007/s10558-009-9089-9

ORIGINAL PAPER

Hemodynamic Environments from Opposing Sides of Human Aortic Valve Leaflets Evoke Distinct Endothelial Phenotypes In Vitro

Eli J. Weinberg · Peter J. Mack · Frederick J. Schoen · Guillermo García-Cardeña · Mohammad R. Kaazempur Mofrad

Published online: 28 January 2010

Abstract The regulation of valvular endothelial phenotypes by the hemodynamic environments of the human aortic valve is poorly understood. The nodular lesions of calcific aortic stenosis (CAS) develop predominantly beneath the aortic surface of the valve leaflets in the valvular fibrosa layer. However, the mechanisms of this regional localization remain poorly characterized. In this study, we combine numerical simulation with in vitro experimentation to investigate the hypothesis that the previously documented differences between valve endothelial phenotypes are linked to distinct hemodynamic environments characteristic of these individual anatomical locations. A finite-element model of the aortic valve was created, describing the dynamic motion of the valve cusps and blood in the valve throughout the cardiac cycle. A fluid mesh with high resolution on the fluid boundary was used to allow accurate computation of the wall shear stresses. This model was used to compute two distinct shear stress waveforms, one for the ventricular surface and one for the aortic surface. These waveforms were then applied experimentally to cultured human endothelial cells and the expression of several pathophysiological relevant genes was assessed. Compared to endothelial cells subjected to shear stress waveforms representative of the aortic face, the endothelial cells subjected to the ventricular waveform showed significantly increased expression of the "atheroprotective" transcription factor Kruppel-like factor 2 (KLF2) and the matricellular protein Nephroblastoma overexpressed (NOV), and suppressed expression of chemokine Monocyte-chemotactic protein-1 (MCP-1). Our observations suggest that the difference in shear stress waveforms between the two sides of the aortic valve leaflet may contribute to the documented differential side-specific gene expression, and may be relevant for the development and progression of CAS and the potential role of endothelial mechanotransduction in this disease.

Keywords Aortic valve · Calcific aortic stenosis · Endothelial mechanotransduction · Shear stress · Cell mechanics and mechanotransduction · Valvular disease

E. J. Weinberg (✉) · M. R. Kaazempur Mofrad
Department of Bioengineering, University of California, Berkeley, CA 94720, USA
e-mail: eli.alum@alum.mit.edu

E. J. Weinberg · P. J. Mack
Department of Mechanical Engineering, Massachusetts Institute of Technology, Cambridge, MA, USA

P. J. Mack · F. J. Schoen · G. García-Cardeña
Department of Pathology, Brigham and Women's Hospital and Harvard Medical School, Boston, MA 02115, USA

P. J. Mack · F. J. Schoen
Harvard-MIT Division of Health Sciences and Technology, Cambridge, MA, USA

Introduction

Aortic stenosis is the most frequent heart valve disease in developed countries and has significant clinical implications for those affected (Carabello and Paulus 2009). Early lesions are prevalent in adults of all age groups (Kuusisto et al. 2005), with early calcific sclerosis present in 20–30% of individuals over 65 years and 48% of those over 85 years (Carabello and Paulus 2009; Otto et al. 1999). In CAS, these lesions form large calcific nodules which can severely impair valve function. Clinically significant stenosis affects 2% of individuals over 65 years and 4% over 85 (Carabello

and Paulus 2009). The first stage of CAS, aortic valve sclerosis, is characterized by the appearance of lesions similar in some respects to those of atherosclerosis (Kuusisto et al. 2005; Otto et al. 1994). Both the initial lesions and calcified nodules develop predominantly in the fibrosa, the collagenous layer of the valve leaflet below the aortic surface (Kuusisto et al. 2005; Otto 2003; Thubrikar 1990). The initial calcific lesions are nucleated in the valvular interstitial cells (VIC) (Kim and Huang 1971; Kim et al. 1976). CAS is likely potentiated by the effects of biomechanical forces acting on the valvular endothelial cells (VEC) and/or the VIC, but it remains unknown how each cell type is affected and whether the key disease-inducing forces are solid deformations (Robicsek et al. 2004), hemodynamic shear forces (Butcher and Nerem 2007), or a combination of the two. The current understanding of these effects and their interplay has recently been reviewed (Schoen 2008). Our recent efforts have used computational models to demonstrate the uncertainty of linking cell-scale deformations to CAS processes (Weinberg and Kaazempur-Mofrad 2008). In that work, we investigated the multiscale mechanical deformations in the normal (tricuspid) aortic valve and the bicuspid aortic valve. We showed that, while organ-scale deformations were different between the tricuspid and bicuspid valve, differences in cell-scale deformations were small and could not explain the difference in calcification between the two valves. Here, we use numerical models, in combination with in vitro cellular approaches, to generate side-specific aortic valve hemodynamic shear stress waveforms and investigate the link between these specific waveforms and the endothelial phenotypes they evoke.

It is well established that hemodynamic forces acting along the endothelium differ between the two sides of the aortic valve leaflet (Weston et al. 1999; Einav et al. 1989), leading some to hypothesize that the side-specific nature of CAS may arise from flow-mediated differences in aortic valve endothelial cell phenotypes. In support of this hypothesis, studies from explanted porcine aortic valves and cultured porcine aortic valve endothelial cells have demonstrated that the two sides of the leaflet display marked differences in expression of genes specific to vasorelaxation, inflammation, and bone-deposition processes, including C-natriuretic peptide (CNP) and bone morphogenic protein 4 (BMP-4) (Simmons et al. 2005; Butcher et al. 2006). The goal of this study was to generate physiologically relevant shear stress waveforms exhibited by the aortic valve and show that these specific waveforms can influence side-dependent endothelial gene expression. Constructing a reliable experimental measurement of the dynamic shear profiles in the valve, however, has proven difficult to-date. For example, the reported peak shear stresses acting along the valve surface range from 29 to 1,200 dynes/cm^2 (Weston et al. 1999; Einav et al. 1989). To better characterize the valvular flow patterns, we created a computational model of the human aortic valve hemodynamics and calculated the transient shear stress waveforms that act on each side of the aortic valve. These distinct, pulsatile waveforms were then applied to cultured human endothelial cells and differences in endothelial expression of genes previously correlated with vascular inflammation and atherogenesis were observed. Our results identify a connection between the shear stress experienced by aortic valve endothelium and endothelial gene expression and function that may play a role in the mechanism of aortic stenosis, suggesting a potential role for shear-induced endothelial mechanotransduction (Davies and Helmke 2009; Mofrad and Kamm 2009). More specifically, the shear stress profile calculated from our aortic valve model, when applied to human umbilical vein endothelial cells in vitro, resulted in differing expression in 3 of 4 genes studied.

Methods

Computational Model

To accurately calculate the shear waveforms applied to each side of the aortic valve leaflet, we created a 2-dimensional fluid-structure numerical simulation of the human aortic valve. This model is a simplified version of the 3-dimensional simulation we have previously described (Weinberg and Kaazempur Mofrad 2007), but with high resolution on the fluid boundary to accurately resolve the wall shear stress patterns. Our previous model uses the operator-split method to handle fluid-structure interactions, where the deforming solid passes through a stationary fluid mesh. With operator-split, accurate calculation of the momentum boundary layers requires high resolution throughout the fluid mesh, and thus high computational cost. In order to resolve the momentum boundary layers and accurately compute the shear stress applied to the valve surfaces, we modified the previous model by employing the Arbitrary Lagrangian–Eulerian (ALE) method. With ALE, a fine fluid mesh remains attached to the solid boundaries while mesh in the bulk can be coarser. Geometries of the solid and fluid were created in SolidWorks (SolidWorks, Concord, MA) based on experimental measurements of overall valve geometry (Thubrikar 1990) and of thickness at various locations on the cusp (Grande-Allen et al. 2001). The full 3-dimensional geometry is shown in Fig. 1a, with a cutaway showing a plane of symmetry along the center of a leaflet. The solid and fluid geometry in that plane are the 2-dimensional geometries for the current model. Geometry was meshed in ADINA (ADINA R&D, Watertown, MA). Both the solid and fluid phases were meshed with 3-node triangular elements. To permit large displacements of the solid, the Arbitrary

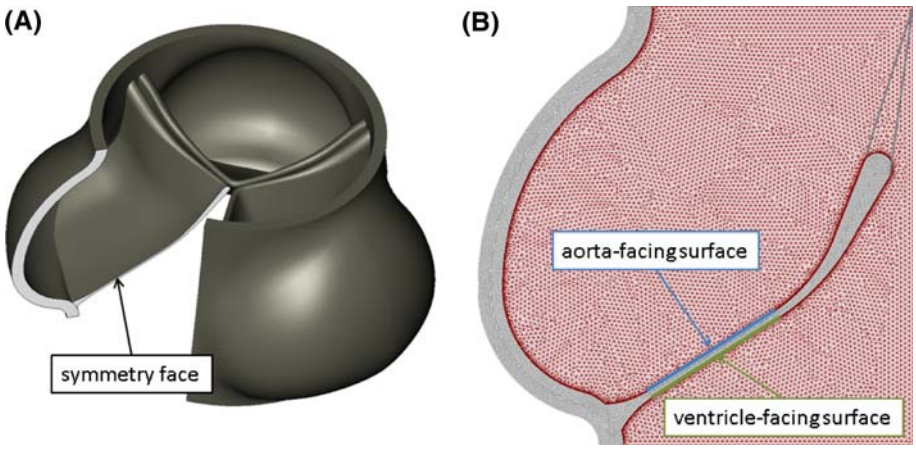

Fig. 1 Aortic valve geometries. **a** Full 3-d geometry, created in CAD software based on experimental measurements, showing symmetry plane and **b** Meshed 2-dimensional simulation geometry. Aortic and ventricular surfaces are illustrated

Lagrangian–Eulerian (ALE) method with remeshing of the fluid was used. The solid phase was modeled with an exponential Mooney-Rivlin material model with constants fit to experimental data (Weinberg and Kaazempur Mofrad 2007; Billiar and Sacks 2000a, b) ($D_1 = 1{,}000$ Pa, $D_2 = 30$) and blood modeled as a Newtonian fluid ($\mu = 0.003$ Pa s). Spring elements with a locking stretch of $\lambda = 1.25$ were added to represent the effect of the connection of tissue between the center of the leaflet and the commissures. Simulation geometry, including the solid phase, fluid phase, and added spring elements, is illustrated in Fig. 1b. The simulation was run in ADINA, subject to dynamic pressure boundary conditions (Weinberg and Kaazempur Mofrad 2007). The model was verified by comparing computed results to experimental data for flow rate, peak fluid velocity, and cusp displacement using previously described verification techniques (Weinberg and Kaazempur Mofrad 2007). Shear profiles applied to the aortic and ventricular surfaces were recorded versus time for one cardiac cycle and averaged over the locations shown in Fig. 1b.

Shear Stress Application

The two computed shear waveforms were applied to cultured endothelial cells using a cone-and-plate dynamic flow system (DFS), as previously described (Dai et al. 2004). Briefly, the DFS rotates a modified cone over a plate seeded with a confluent monolayer of endothelial cells. The cone is driven by a computer-controlled stepper motor (Zeta6104, Axis New England). The design parameters (e.g., cone angle, plate diameter, and medium viscosity) had been evaluated to ensure that the flow is laminar, and that the shear stress is directly proportional to the angular velocity of the cone. Precise control of the cone rotation therefore allows the device to simulate various shear stress waveforms. For each set of experiments, two identical flow devices were used simultaneously. One of them was programmed to simulate the aortic side waveform, whereas the other was used for the ventricular waveform (Fig. 2).

Human Endothelial Cell Culture

Human umbilical vein endothelial cells (HUVEC) were isolated and maintained as previously described (Dai et al. 2004). Briefly, HUVEC (passage 1) were plated on 0.1% gelatin (Difco)-coated polystyrene circular plates (Plaskolite) at a density of 60,000 cells/cm^2 and maintained at 37°C and 5% CO_2 in Medium-199 (BioWhittaker) supplemented with 50 μgμ/ml endothelial cell growth supplement (Collaborative Research) 100 μg/ml heparin (Sigma), 100 U/ml penicillin plus 100 μg/ml streptomycin (BioWhittaker), 2 mM L-Glutamine (Gibco), and 20% FBS (BioWhittaker). After 24 h, the plate was assembled in the DFS and the HUVEC monolayers were exposed to the aortic and ventricular waveforms using the medium described above with an additional 2% wt/v dextran (Invitrogen) in order to achieve a fluid viscosity of 2.15 cP. The waveforms were applied for 24 h, over which interval the medium was exchanged at a rate of 0.05 ml/min. The 24-h time point was selected for comparison between waveforms to allow transient changes in transcription that primarily reflect the step-like transition from the static condition to a fluid dynamic culture condition to subside, which has previously been used as a steady-state approximation for characterizing flow-dependent endothelial phenotypes (Garcia-Cardena et al. 2001).

RNA Isolation and Gene Expression Measurement

Total RNA was isolated using Lysis Buffer (Applied Biosystems) and purified using the Prism Nucleic Acid Prep-Station (Applied Biosystems) according to the manufacturer's instructions. RNA quantity was measured by spectrophotometic analysis at 260 nm and quality was verified by

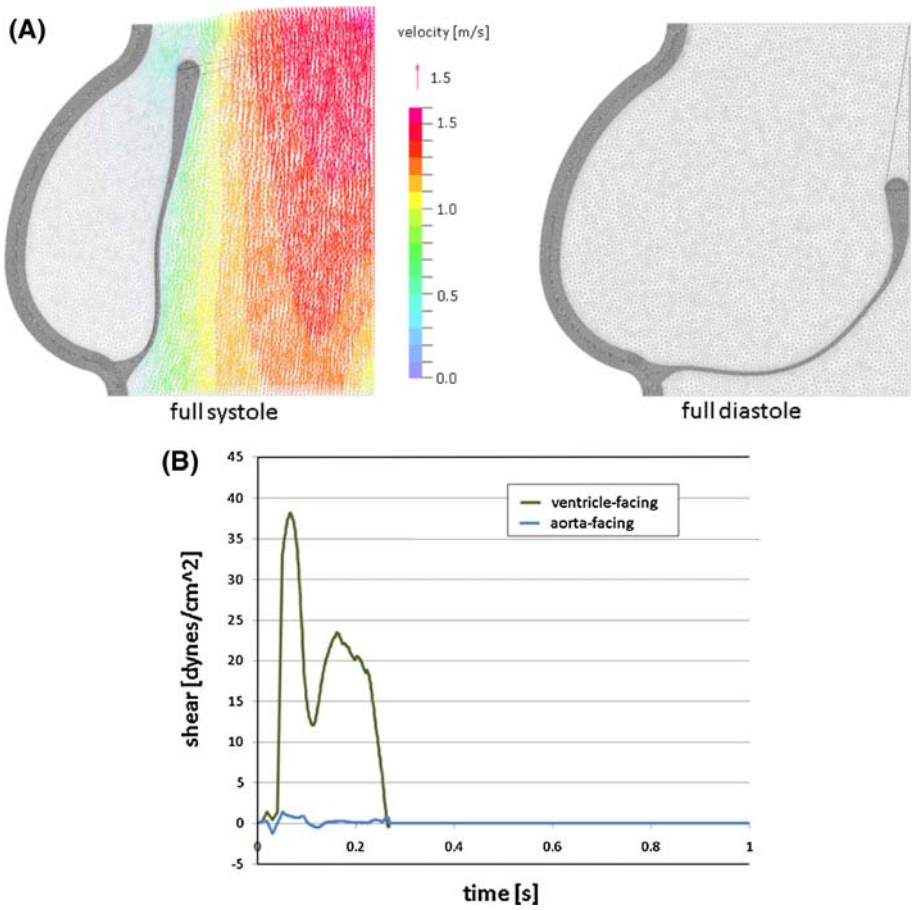

Fig. 2 Results of numerical simulation. **a** Deformed geometries and fluid velocity profiles in systole and diastole and **b** shears recorded for typical locations on aortic and ventricular surfaces

Agilent's 2100 Bioanalyzer with RNA 6000 Nano LabChip Kit. Purified, DNase-treated RNA (0.5 μg) was reverse-transcribed using a MultiScribe-based 25 μl reaction (Applied Biosystems). The cDNA was diluted in 50 μl DNAse-free water and subjected to a 20 μl real-time TaqMan quantitative PCR (Applied Biosystems 7900). Expression of Kruppel-like Factor 2 (KLF2, TaqMan probe Hs00360439_g1), Nephroblastoma Overexpressed (NOV, TaqMan probe Hs00159631_m1), Monocyte Chemoattractant Protein 1 (MCP-1/CCL2, TaqMan probe Hs00234140_m1), and VE-Cadherin (CDH5, TaqMan probe Hs00174344_m1) were reported relative to GAPDH (TaqMan probe Hs99999905_m1) and normalized to aortic expression levels. The data reported represents the mean of three independent experiments with the error bars representing standard error. Differences were considered statistically significant for $P < 0.01$, as determined by one-way ANOVA (Primer of Statistics).

Results

Numerical simulations of the biomechanical forces acting on the aortic valve were run to convergence for one full cardiac cycle, yielding deformed geometries and fluid velocity profiles (Fig. 2a). Bulk velocity profiles match those of our previous models and experimental data (Thubrikar 1990; Weinberg and Kaazempur Mofrad 2007), and finely resolved velocities at the fluid boundaries were used to extract time-varying shear waveforms for each face of the valve (Fig. 2b). The ventricular waveform reached higher magnitudes (40 dynes/cm^2 maximum, an average of 4.7 dynes/cm^2 over the cardiac cycle), and does not exhibit flow-reversal, while the aortic waveform contains significantly lower magnitudes (3 dynes/cm^2 maximum, an average of 0.07 dynes/cm^2 over the cardiac cycle) with flow-reversal. The computed hemodynamic waveforms, however, are notably different from others that have been used to investigate the effect of shear forces on endothelial phenotype (Dai et al. 2004). In the systemic vasculature, arterial shear forces have a time-varying component, but typically remain non-zero throughout the cardiac cycle. In contrast, the aortic valve experiences a spike in shear during systole when the valve is open and blood is being ejected from the left ventricle and zero shear during diastole when the valve is closed, as reflected in the simulated valve waveforms (see Fig. 2).

Application of the simulated aortic valve waveforms to cultured HUVEC, a primary endothelial cell that has been previously shown to display significant plasticity when exposed to shear stress in culture for 24 h (Dai et al. 2004; Garcia-Cardena et al. 2001; McCormick et al. 2001; Chen et al. 2001) resulted in the differential expression of endothelial genes that regulate vascular homeostasis and may be important for the initiation and progression of CAS. In particular, HUVEC exposed to the ventricular valve waveform displayed an increase in the expression of the vasoprotective transcription factor KLF2 and the matricellular protein NOV, as well as decreased expression of pro-inflammatory molecule MCP-1. There was no change in the pan-endothelial marker VE-Cadherin in cells exposed to the ventricular valve waveform compared to the aortic waveform (see Fig. 3).

Discussion

CAS represents an important pathological state of cardiac valves. Valvular interstitial cells develop calcific deposits, which eventually coalesce, leading to macroscopic calcified nodules, some lesions evolve in the context of an inflammatory focus that resembles the lesions of atherosclerosis.

How the extent of valve leaflet calcification may directly contribute to stenosis, both in terms of changes in mechanical properties and increased viscous load, is of clinical significance. As the aortic heart valve undergoes geometric and mechanical changes over time, the cusps of a normal, healthy valve thicken and become less extensible over time. In the disease calcific aortic stenosis, calcified nodules progressively stiffen the cusps. The local mechanical changes in the cusps, due to either normal aging or pathological processes, affect overall function of the valve. We recently proposed a computational model for the aging aortic valve that connects local changes to overall valve function (Weinberg et al. 2009). To model normal/uncomplicated aging, leaflet thickness and extensibility were varied versus age according to experimental data. To model calcification, initial sites were defined and a simple growth law was assumed. The nodules then were allowed to grow over time, increasing the area of calcification representing greater age. This model provides a framework for linking overall valve function to valve mechanical properties and geometry, capturing the valve narrowing and increase in fluid velocity seen in patients (Weinberg et al. 2009). The ability to better understand and predict disease progression will aid in design and timing of patient treatments for CAS.

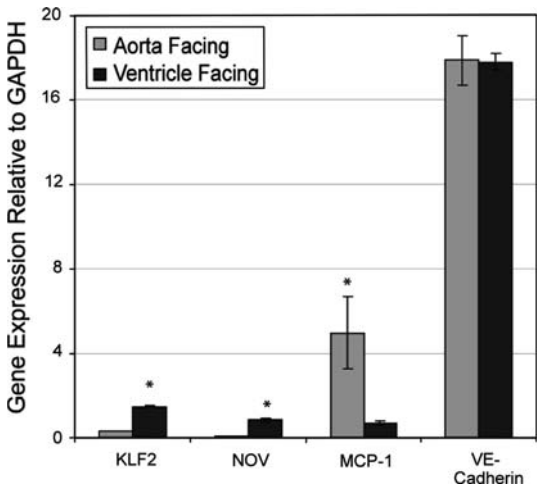

Fig. 3 Ventricular aortic valve waveforms evoke an anti-inflammatory endothelial phenotype, as assessed by KLF2, NOV, and MCP-1 gene expression. VE-Cadherin expression, a pan-endothelial marker, showed no difference in expression between the two flow patterns. Data is the average of 3 independent experiments with the *error bars* representing ± the standard error. * $P < 0.01$, as determined by one-way ANOVA. KLF2 = Kruppel-like Factor 2; NOV = Nephroblastoma Overexpressed; MCP-1 = Monocyte Chemoattractant Protein 1

While the clinical importance of CAS is well established, the cellular and molecular mechanisms leading to this pathogenesis remain unknown. In particular, the effect the hemodynamic environment has on valvular cells, as well as the valve structure and function, has gained recent attention (Simmons et al. 2005). In this study, we developed a finite element fluid-structure simulation of the aortic valve motion, with high resolution at the fluid boundary, in order to extract the shear waveforms applied by the blood to the aortic and ventricular valve endothelium. This methods allows us, for the first time, to describe the specific shear waveforms to which the two sides of the aortic valve cusp are subjected, and thus to recreate the specific hemodynamic environment of the valve surfaces in vitro. The simulated waveforms (Fig. 2) were applied to cultured human endothelial cells in order to investigate whether these waveforms influence endothelial gene expression. Using this in vitro model, the cells exposed to the ventricular waveform were found to display an anti-inflammatory endothelial molecular phenotype, as determined by the increased expression of KLF2 and NOV, as well as the suppression of MCP-1, compared to cells exposed to the waveform from the aortic side of the leaflet.

Previous studies have shown that endothelial KLF2 mutes the expression of genes associated with vascular inflammation, thrombosis, and calcification in the context of pro-inflammatory stimuli. These pathophysiological processes are linked to atherogenesis, and may also be relevant to the pathogenesis of CAS (Parmar et al. 2006). One of the factors suppressed by KLF2 is bone morphogenic protein 4 (BMP4), a gene shown by others to display valve leaflet side-dependent expression (Butcher and Nerem 2007; Simmons et al. 2005; Butcher et al. 2006).

NOV and MCP-1 have both previously been shown to be targets of KLF2 in the context of flow-mediated vasoprotection (Parmar et al. 2006), however, the role of NOV in the human aortic valve has yet to be defined.

The data presented here should be viewed in the context of our current knowledge of endothelial phenotypes in the valve and the relationship between those phenotypes and flow. Studies in this field have only recently begun. Simmons et al. (2005) demonstrated side-specific differential expression of 584 genes in explanted pig cusp tissue, representing the steady-state phenotypes of the healthy valve. Butcher et al. (2006), on the other hand, exposed pig aortic and valvular endothelial cells to steady shear stress for 48 h and observed both similarities and differences in how flow affects gene expression in these distinct cell types. Our current work shows that human umbilical vein endothelial cells exposed to the different shear waveforms of the valve display different phenotypes, suggesting that endothelial mechanotransduction may be important in defining the previously documented in vivo gene expression (Simmons et al. 2005; Davies and Helmke 2009; Mofrad and Kamm 2009). Importantly, the work of Butcher et al. shows that valvular endothelial cells respond differently to shear stress when compared to other endothelial cells. Thus, our work is limited by use of HUVEC, a primary endothelial cell culture from venous origin. However, despite this limitation our study clearly demonstrates the phenotypic plasticity of HUVEC in the context of cardiac valve-derived hemodynamic environments. Further studies with valvular endothelial cells are required to determine the orchestrated response of those cells to shear stress. An additional limitation of current work in the field is that all results have been obtained from non-pathologic valves. While the phenotypes of the healthy valve can suggest susceptibility to disease, gene expression during transition to pathologic states has not yet been studied.

This work constitutes evidence supporting the hypothesis that hemodynamic forces may act as important determinants of the different endothelial phenotypes observed on the two sides of the aortic valve cusp. This difference in phenotype may subsequently drive the side-specific nature of lesion formation in CAS. Further efforts to recognize the specific molecular determinants of the process in the valve may ultimately enhance understanding of the disease and design of therapies for CAS.

Sources of Funding EW was supported by a Draper Fellowship and PM by the Molecular, Cellular, and Tissue Biomechanics NIH training grant (T32 EB006348). This work was partially supported by the NIH (NHLBI) (G.G-C RO1-HL7066686).

Disclosures The funders had no role in study design, data collection and analysis, decision to publish, or preparation of the manuscript.

References

Billiar K, Sacks MS. Biaxial mechanical properties of the natural and glutaraldehyde treated aortic valve cusp-part I: experimental results. J Biomech Eng. 2000a;122:23–30.

Billiar K, Sacks MS. Biaxial mechanical properties of the natural and glutaraldehyde treated aortic valve cusp-part II: a structural constitutive model. J Biomech Eng. 2000b;122:327–35.

Butcher J, Nerem RM. Valvular endothelial cells and the mechanoregulation of valvular pathology. Phil Trans R Soc B. 2007; 362:1445–57.

Butcher J, Tressel S, Johnson T, Turner D, Sorescu G, et al. Transcriptional profiles of valvular and vascular endothelial cells reveal phenotypic differences—influence of shear stress. Arterioscler Thromb Vasc Biol. 2006;26:69–77.

Carabello BA, Paulus WJ. Aortic stenosis. Lancet. 2009;373:956–66.

Chen B, Li Y, Zhao Y, Chen K, Li S, et al. DNA microarray analysis of gene expression in endothelial cells in response to 24-h shear stress. Physiol Genomics. 2001;7:55–63.

Dai G, Kaazempur-Mofrad MR, Natarajan S, Zhang Y, Vaughn S, Blackman BR, Kamm RD, García-Cardeña G, Gimbrone MA Jr. Distinct endothelial phenotypes evoked by arterial waveforms derived from atherosclerosis-susceptible and -resistant regions of human vasculature. PNAS. 2004;101:14871–6.

Davies PF, Helmke BP. Endothelial mechanotransduction. In: Mofrad MRK, Kamm RD, editors. Cellular mechanotransduction: diverse perspectives from molecules to tissues. New York, NY: Cambridge University Press; 2009.

Einav S, Stolero D, Avidor J, Elad D, Talbot L. Wall shear stress distribution along the cusp of a tri-leaflet prosthetic valve. J Biomed Eng. 1989;12:13–8.

Garcia-Cardena G, Comander J, Anderson K, Blackman B, Ma G. Biomechanical activation of vascular endothelium as a determinant of its functional phenotype. PNAS. 2001;98:4478–85.

Grande-Allen K, Cochran R, Reinhall P, Kunzelman K. Finite-element analysis of aortic valve sparing: influence of graft shape and stiffness. IEEE Trans Biomed Eng. 2001;48:647–59.

Kim KM, Huang SN. Ultrastructural study of calcification of human aortic valve. Lab Invest. 1971;25:357–66.

Kim KM, Valigorsky JM, Mergner WJ, Jones RT, Pendergrass RF, et al. Aging changes in the human aortic valve in relation to dystrophic calcification. Hum Pathol. 1976;7:47–60.

Kuusisto J, Rasanen K, Sarkioja T, Alarakkola E, Kosma V. Atherosclerosis-like lesions of the aortic valve are common in adults of all ages: a necropsy study. Heart. 2005;91:576–82.

McCormick S, Eskin S, McIntire L, Teng C, Lu C, et al. DNA microarray reveals changes in gene expression of shear stressed human umbilical vein endothelial cells. PNAS. 2001;98:8955–60.

Mofrad MRK, Kamm R. editors. Cellular mechanotransduction: diverse perspectives from molecules to tissues. New York, NY: Cambridge University Press; 2009.

Otto CM. Valvular heart disease. 2nd ed. Philadelphia: Saunders; 2003.

Otto CM, Kuusisto J, Reichenbach D, Gown A, O'Brien K. Characterization of the early lesion of degenerative valvular aortic-stenosis—histological and immunohistochemical studies. Circulation. 1994;90:844–53.

Otto C, Lind B, Kitzman D, Gersh B, Siscovick D. Association of aortic-valve sclerosis with cardiovascular mortality and morbidity in the elderly. N Engl J Med. 1999;341:142–7.

Parmar K, Larman H, Dai G, Zhang Y, Wang E, et al. Integration of flow-dependent endothelial phenotypes by Kruppel-like factor 2. J Clin Invest. 2006;116:49–58.

Robicsek F, Thubrikar MJ, Cook JW, Reames MK, Fowler BL, et al. Creases and folds: why does the bicuspid aortic valve fail so early? J Am Coll Cardiol. 2004;43:436A.

Schoen F. Evolving concepts of cardiac valve dynamics: the continuum of development, functional structure, pathobiology, and tissue engineering. Circulation. 2008:1864–80.

Simmons C, Grant G, Manduchi E, Davies P. Spatial heterogeneity of endothelial phenotypes correlates with side-specific vulnerability to calcification in normal porcine aortic valves. Circ Res. 2005;96:792–9.

Thubrikar M. The aortic valve. Boca Raton: CRC Press; 1990.

Weinberg EJ, Kaazempur Mofrad MR. Transient, three-dimensional, multiscale simulations of the human aortic valve. Cardiovasc Eng. 2007;7:140–55.

Weinberg EJ, Kaazempur-Mofrad M. A multiscale computational comparison of the bicuspid and tricuspid aortic valves in relation to calcific aortic stenosis. J Biomech. 2008;41:3482–7.

Weinberg EJ, Schoen FJ, Mofrad MR. A computational model of aging and calcification in the aortic heart valve. PLoS One. 2009;4(6):e5960.

Weston M, LaBorde D, Yoganathan AP. Estimation of shear stress on the surface of an aortic valve leaflet. Ann Biomed Eng. 1999; 27:572–9.